Phase Transition Models based on A N-Body Complex Statistics

David C. Ni

***Abstract*—Ginzburg-Landau theories and Topological Phase Transition theories are developed in the different theoretical frameworks remarked as effective theories for different types of phase transitions, such as symmetry breaking and continuous phase transitions. Our framework based on Nonlinear Lorentz Transformation demonstrates nonlinear to linear degeneracy and continuum to discreteness transition, therefore motivate us to extend for the unification of the existing theories.**

***Index Terms*—Blaschke, Conjugate Symmetry, Lorentz, Nonlinear, Relativity.**

I. Introduction

Recently theories and applications of topological order have attracted significant attentions in the areas of condensed-matter physics as well as in other branches of mathematics and physics. This long-range quantum entanglement is currently recognized as a mechanism, which is neither spontaneous symmetry breaking, nor related to traditional theories, such as order-parameter phase transitions and quasi-particle in Ginzburg-Landau theory [1]. Current efforts are toward to establish models for unifying both gapped and gapless states. A more general and perspective mathematical framework is definitely expected for unifying these topological theories [2] with the traditional ones.

Fundamentally the efforts on unification of topological order and traditional unification will certainly encounter the development of mechanisms for the transitions of the continuous bulk states and the discrete edge states, i.e., the bulk-edge correspondence. We are hereby motivated to further extend a mathematical construction, which demonstrates parameter-dependant topological transitions from continuous sets to discrete sets in the momentum space. The construction is based on a global function in the form of extended Blaschke functions [3] and equations, which represent a nonlinear extension of Lorentz transformation. In addition, we include a local function in the form of a phase evolution, $exp(-i\psi)$. This construction establishes a normalized momentum space – the complex plane. A point on the complex plane represents a normalized state of particle momentum observed from a reference frame in the theory of special relativity. The construction includes an internal energy structure for a particle in the ensemble, and mainly intends to approach the N-body problem using nonlinearity instead of perturbation [4-10].

Manuscript received March 17, 2013. D. C. Ni is with Direxion Technology, Taipei, Taiwan, 106 R.O.C., (corresponding author to provide phone: 886-2-23511832; fax: 886-2-2394-6023; e-mail: davidcni@ yahoo.com).

Based on the observations of numerical analysis on the constructed meromorphic functions, we classify three types of parameter-depended topological transitions in conjunction with normalized momentum. The first type is analogue to the order-parameter phase transition, while the second and third types are related to the continuous phase transitions. These types show topological degeneracy and transitions in conjunction with genus of a toroidal system with fractal structures. Vortex structures at fraction-valued points on the complex plane are also observed. The richness of the observed structures manifests the construction as initially a potential mathematical framework for theoretical unification of topological order and traditional statistical theories.

II. Construction of Functions and Equations

A. Functions and Equations

Given two inertial frames with different velocities, u and v, the observed velocity, u', from v-frame is as follows:

$$u' = (u - v) / (1 - vu/c^2) \tag{1}$$

We set $c^2 = 1$ and the multiply a phase connection, $exp(i\psi(u))$, to the normalized complex form of the equation (1) based on the concept of gauge transformation as follows:

$$(u'/u) = exp(i\psi(u))(1/u)[(u-v)/(1-uv)] \tag{2}$$

We hereby define a generalized complex function under consideration of phase connection, $exp(i\psi(u))$ as follows:

$$f_{B,}(z,m) = z^{-1}\Pi^m C_i \tag{3}$$

And C_i has the following forms:

$$C_i = exp(g_i(z))[(a_i-z)/(1-\bar{a}_i z)] \tag{4}$$

Where z is a complex variable representing the velocity u, a_i is a parameter representing velocity v, $\bar{a}_i$ is the complex conjugate of a complex number a_i and m is an integer. The term $g_i(z)$ is a complex function assigned to $\Sigma^p 2p\pi iz$ with p as an integer. The degree of $f_B(z,m) = P(z)/Q(z)$ is defined as Max{deg P, deg Q}.

The function f_B is called an extended Blaschke function (EBF) [3]. The extended Blaschke equation (EBE) is defined as follows:

$$f_B(z,m) - z = 0 \tag{5}$$

B. Original and Mapped Domains

A domain can be the entire complex plane, C_∞, or a set of complex numbers, such as $z = x+yi$, with $(x^2 + y^2)^{1/2} \square R$, and R is a real number. For solving the EBE and ELE, a function f will be iterated as:

$$f^n(z) = f \circ f^{n-1}(z), \tag{6}$$

Where n is a positive integer indicating the number of iteration. The function operates on a domain, called original domain. The set of $f^n(z)$ is called mapped domain. In the figures, the regions in black color represent stable Fatou sets containing the convergent points of the concerned equations and the white (i.e., blank) regions correspond to Julia sets, the complementary sets of Fatou sets on C_∞.

C. Parameter Space

In order to characterize the original and the mapped domains, we define a set of parameters called parameter space. The parameter space includes six parameters: 1) z, 2) a, 3) *exp(gi(z))*, 4) m, 5) *iteration*, and 6) *degree*. In the context of this paper we use the set {*z, a, exp(gi(z)), m, iteration, degree*} to represent this parameter space. For example, {*a*}, is one of the subsets of the parameter space.

D. Conformal Mapping and Fractal

On the complex plane, the convergent domains of the functions form fractal patterns of with limited-layered structures, which demonstrate skip-symmetry, symmetry broken, chaos, and degeneracy in conjunction with parameter space [7].

Figure 1(a) and 1(b) show the original and the mapped domains of $f_B(z,m)$ of 11th degree respectively. Both domains are at scale of 10^{10}. This Figure shows a conformal mapping from the original domain to the mapped domain.

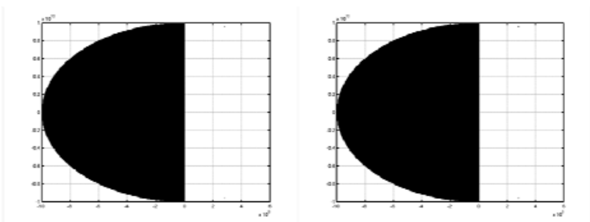

(a) Original Domain (b) Mapped Domain

Fig. 1 (a) Original Domain and (b) Mapped domain of $f_B(z,10)$.

Figure 2 shows two types of fractal patterns of original domains. These patterns are plots at different scales. In order to demonstrate these figures, we intend to reverse the color tone of Fatou and Julia sets.

Conformal mapping and fractal patterns directly verify that the numerical results are not created from embedded algorithms in the computer architecture.

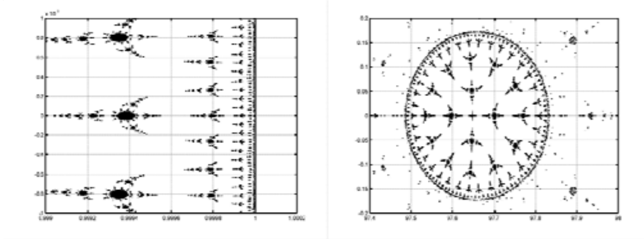

Fig. 2 Fractal Patterns of the Original Domains.

III. Nonlinear to linear degeneracy

Figure 3 shows the Fatou sets of original domains with different degrees and values of parameter {*a*}. Figure 3 (a) through (d) show that the Fatou sets are quite topologically different for different degrees, from $f_B(z,1)$, the linear equation to $f_B(z,4)$. When the value of {*a*} increases from 0.1 to 0.8, The Fatou sets show topologically similar with minor variations as shown from $f_B(z,1)$, the linear equation to $f_B(z,4)$ or even at higher degrees as in Figure 3 (e) through (h). We call this phenomenon as nonlinear-to-linear degeneracy.

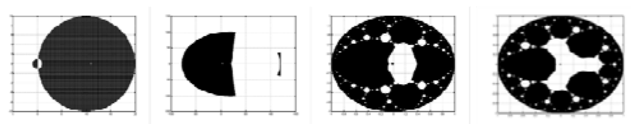

(a) fB(z,1), a=0.1 (b) fB(z,2), a=0.1 (c) fB(z,3), a=0.1 (d) fB(z,4), a = 0.1

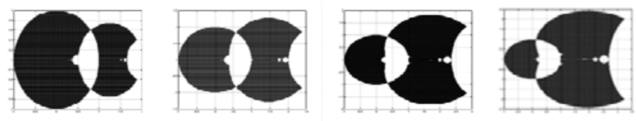

(e) fB(z,1), a=0.8 (f) fB(z,2, a=0.8 (g) fB(z,3), a=0.8 (h) fB(z,4), a = 0.8

Figure 3 Original Domains of $f_B(z,1)$, $f_B(z,1)$, $f_B(z,1)$, and $f_B(z,1)$ with values of {*a*} at 0.1 and 0.8 respectively.

IV. Continuum-to-Discreteness Transition

When the value of {*a*} approaches further to unity, the topological patterns of Fatou sets in original domains demonstrate an abrupt or quantum-type transition from connected sets to discrete sets. The discrete sets show Cantor-like pattern when mapping onto real axes on the complex plane, nevertheless, these sets are not Cantor sets by definition.

The transition of EBF occurs between $a = 1 - 10^{-16}$ and $a = 1 - 10^{-17}$. Figure 4 shows this type of topological transition. Figure 4(a) through 4(d) shows the nonlinear-to-linear degeneracy, and 4(e) shows the Cantor-like pattern at all degrees once the transition occurs. Here, we define $\Delta = 1 - a$. Figure 5 shows another discreteness-to-continuum transition around a pole in original domains based on the parameter {*degree*}.

Figure 6 shows continuum-to-discreteness transitions in mapped domain based on the parameter {*iteration*}. These transitions demonstrate a fabric tori structure of EBF.

ISBN: 978-988-19251-0-7
ISSN: 2078-0958 (Print); ISSN: 2078-0966 (Online)

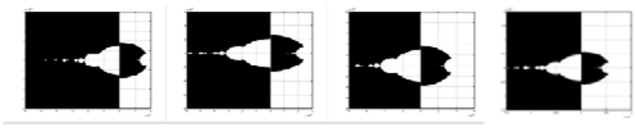

(a) $f_B(z,1)$ (b) $f_B(z,2)$ (c) $f_B(z,3)$ (d) $f_B(z,10)$
All with $\Delta = 10^{-16}$

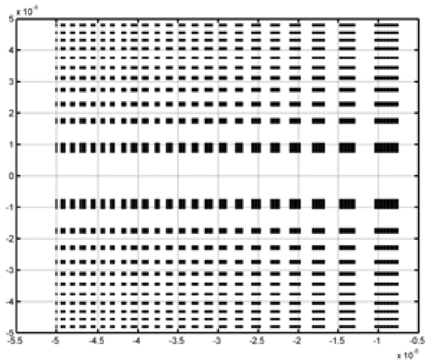

(e) $f_B(z,m)$, $\Delta = 10^{-17}$

Figure 4 Connected sets transit to discrete Cantor-like sets for all $f_B(z,m)$ *at* $\Delta = 10^{-17}$ in original domain.

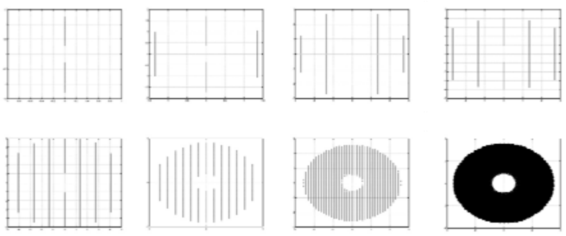

Figure 5 Discreteness to continuum transitions around a pole of EBF as value {*degree*} increases in original domain.

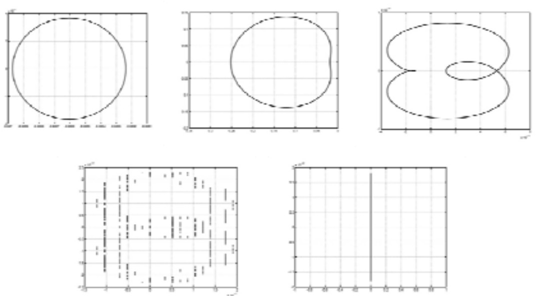

Figure 6 Continuum to discreteness transitions as value {*iteration*} increases in mapped domain.

V. CONJUGATE SYMMETRY

Figure 7 shows a mapping from the convergent Fatou sets of the original domain to the mapped domain. We examine the plots of three different values: absolute, real, and imaginary on the complex plane. The plots of absolute and real values show a modular pattern with 90 degree rotation. These sets are symmetrical to the y-axis, comparing to the x-axis symmetry of the Fatou sets of original domain. However, the plots of imaginary values demonstrate conjugate symmetry to the y-axis. Figure 8 further shows this special feature with different values of *{a}*.

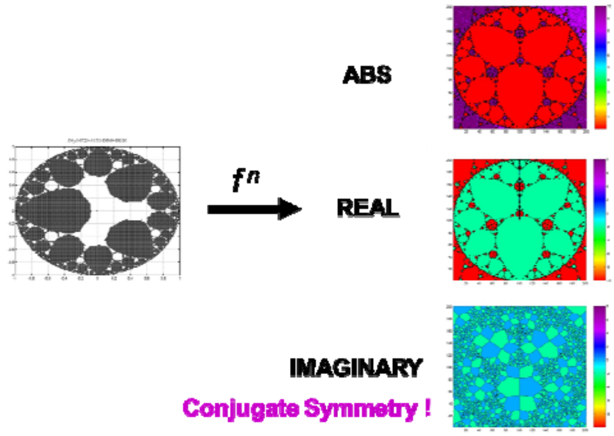

Figure 7 Original Domain

Using the color bar (with $z = 0$ at center of the bar) on the right side of individual figures in Figure 8, we observe the relationship of $z(-x, y) = -z(x, y)$, as so-called conjugate symmetry.

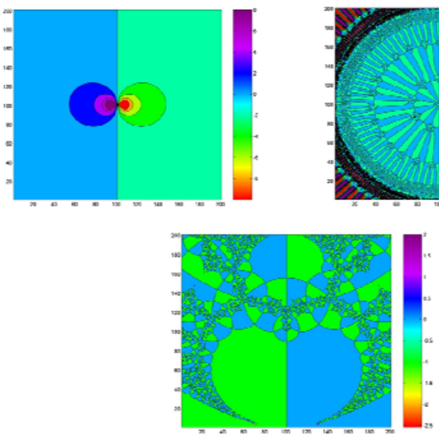

Figure 8 Three patterns of conjugate symmetry at different values of *{a}*.

VI. TYPE I PHASE TRANSITION

Figure 9 shows a set of progressive plot of absolute values of f^{20} as value of *{a}* increases. This transformation manifests an abrupt transition from one fractal pattern to the other pattern.

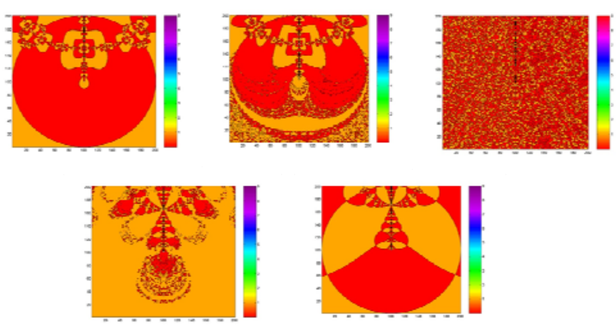

Figure 9 Plots of absolute values of f^{20} as value of *{a}* increases.

Figure 10 shows the plots of real values corresponding to those in the Figure 9. Comparing to the transformation of the plots of the absolute values, the plots of real values show constant without transitions.

ISBN: 978-988-19251-0-7
ISSN: 2078-0958 (Print); ISSN: 2078-0966 (Online)

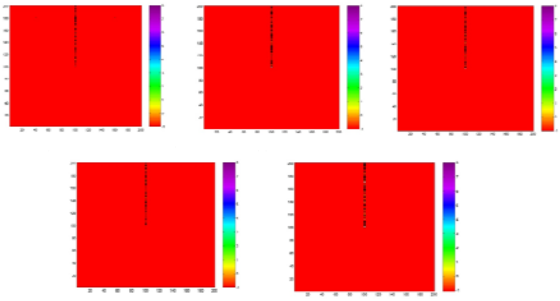

Figure 10 Plots of real values of f^{20} as value of *{a}* increases.

Figure 11 shows the plots of imaginary values corresponding to those in the Figure 9. These plots are directly related to the corresponding absolute ones individually.

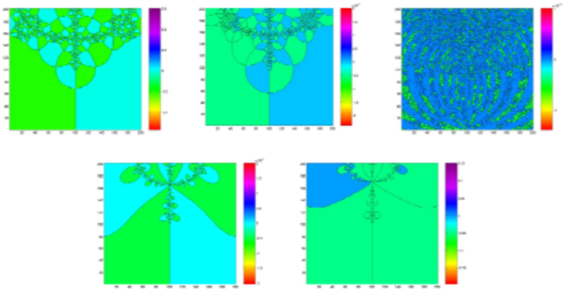

Figure 11 Plots of imaginary values of f^{20} as value of *{a}* increases.

The values of *{a}* in Type I phase transition are in the range of nonlinear-to-linear transition zone as shown in Figure 3. The plots of both absolute and real values maintain symmetry, while the plots of imaginary values show symmetry breaking.

VII. Type II Phase Transition

Figure 12 shows the set of progressive plot of absolute values of f^{10} as value of *{a}* decreases toward value of 0.

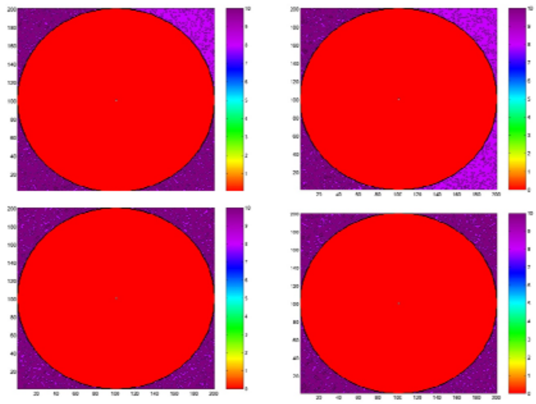

Figure 12 Plots of absolute values of f^{10} as value of *{a}* decreases.

Figure 13 shows the plots of real values corresponding to those in the Figure 12. The patterns show symmetry to the y-axis initially (top-left) and become symmetrical broken locally (bottom-right). Figure 14 shows the plots of imaginary values corresponding to those in the Figure 12. The patterns show conjugate symmetry to y-axis. As the *{a}* decreases, the symmetry is broken. However, symmetry breaking and conjugate-symmetry breaking occur at different value of *{a}*.

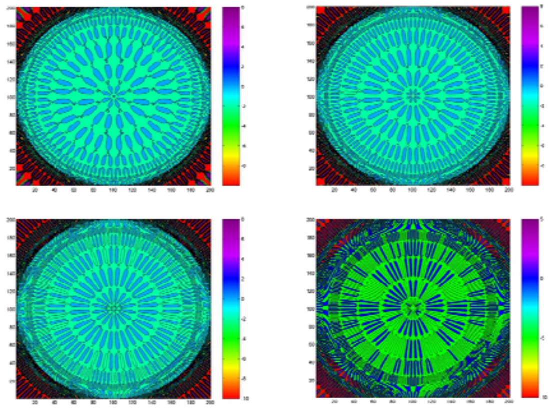

Figure 13 Plots of real values of f^{10} as value of *{a}* decreases

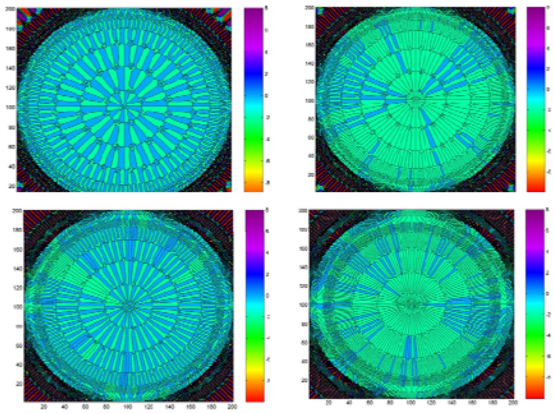

Figure 14 Plots of imaginary values of f^{10} as value of *{a}* decreases

In addition to the symmetry breaking, we also observe that the imaginary values, which are originally in conjugate symmetry, then become the regions with same imaginary value (i.e., same color), namely, in the same phase.

VIII. Type III Phase Transition

Figure 15 shows the set of plot of absolute values of f as value of *{iteration}* increases as the value of *{a}* decreases further. The absolute values, which we propose to be related to the free energy of Ginzburg-Landau theory, are constant to the increase of value of *{iteration}* as well as the value of *{a}*.

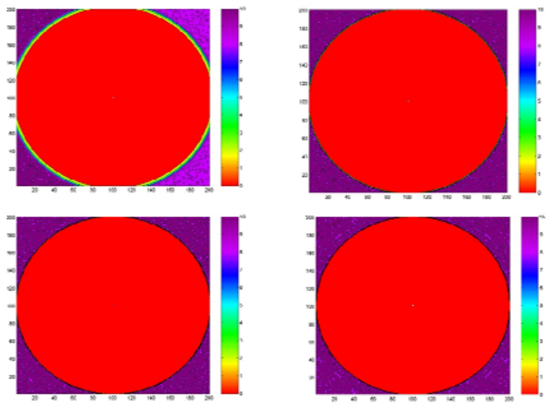

Figure 15 Plots of absolute values of f as value of *{iteration}* increases.

Figure 16 shows the plots of real values corresponding to those in the Figure 15. The patterns show symmetry breaking.

ISBN: 978-988-19251-0-7
ISSN: 2078-0958 (Print); ISSN: 2078-0966 (Online)

In addition, there is a transformation to more complicated patterns of quadrant and higher degree of symmetry. Figure 17 shows the plots of imaginary values corresponding to those in the Figure 15.

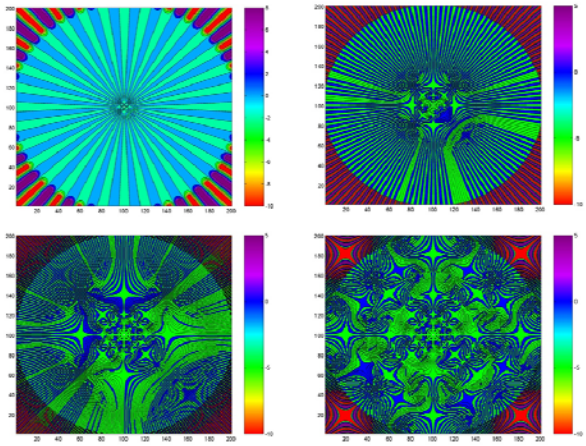

Figure 16 Plots of real values of *f* as value of *{iteration}* increases.

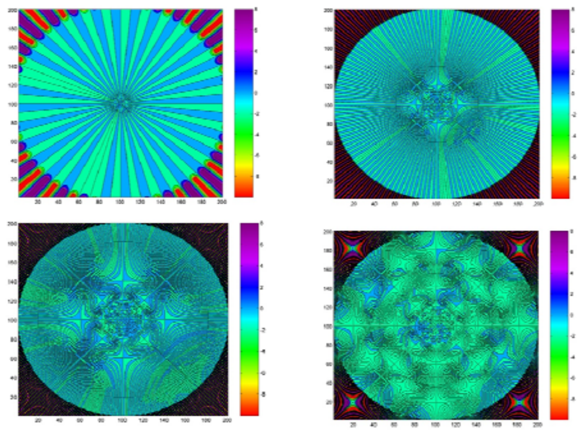

Figure 17 Plots of imaginary values of *f* as value of *{iteration}* increases.

Figure 18 further shows that when further decreasing values of *{a}* and increasing values of *{iteration}*. The imaginary values further converge to the same value, while the real values maintain comparable contrast of adjacent sets.

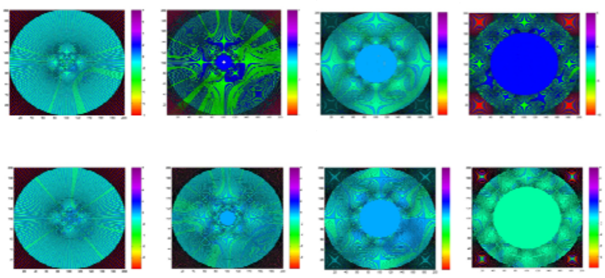

Figure 18 Plots of real values (top row) and imaginary values (bottom row) as values of {a} further approaching to zero.

IX. Conclusion

Our framework provides an additional dimension, phase, which is represented by the imaginary part of the normalized complex momentum. Based on nonlinearity of extended Blaschke function (EBF), which representing nonlinear Lorentz transformation, we observe that the topological transitions, such as nonlinear to linear degeneracy and continuum to discreteness transitions of the dynamically converged fractal sets, i.e., Fatou sets.

Further, we observed two categories of phase transitions, which correspond to the first order, second order, and topological order phase transitions in the conventional classification. The Type I phase transition as classified in this paper, we observe that the absolute values of converged sets transform from one form of symmetry to the second form. In the process of transition, the real values maintain constant, while the imaginary values (i.e., phase) is directly correlated to the absolute values although the Fatou sets of absolute values demonstrate y-axis symmetry, while the Fatou sets of imaginary values demonstrate y-axis conjugate symmetry. Hereby, we relate the absolute values of complex momentum to the free energy in the conventional theories.

The Type II and Type III phase transitions have Fatou sets with constant absolute values, while real values with y-axis symmetry and imaginary values with y-axis conjugate symmetry are coupled to demonstrate symmetry breaking. Further, the Type III demonstrates that the symmetry becomes high-degreed or fractional when the value of the normalized complex momentum approaches to zero.

This theoretical framework based on the concept of nonlinear relativity demonstrates the potential unification of current effective theories, Ginzburg-Landau theories and the theories of topological phase transitions.

Acknowledgment

The author would like to express deep appreciation of support of the family.

References

[1] V.L. Ginzburg and L.D. Landau, *Zh. Eksp. Teor. Fiz.* No. 20, pp. 1064, 1950. English translation in: L. D. Landau, Collected papers (Oxford: Pergamon Press, 1965) p. 546

[2] Xiao-Gang Wen, *Quantum Field Theory of Many Body Systems - From the Origin of Sound to an Origin of Light and Electrons*, Oxford Univ. Press, Oxford, 2004

[3] W. Blaschke, Eine Erweiterung des Satzes von Vitali, "über Folgen analytischer Funktionen" Berichte Math.-Phys. Kl., Sächs. Gesell. der Wiss. Leipzig , No. 67, pp. 194–200, 1915.

[4] D. C. Ni and C. H. Chin, " $Z^1C_1C_2C_3C_4$ *System and Application*", Proceedings of TIENCS workshop, Singapore, August 1-5, 2006.

[5] D. C. Ni, "Chaotic Behavior Related to Potential Energy and Velocity in N-Body Systems", Proceedings of 8th AIMS International Conference on Dynamical Systems, Differential Equations and Applications, May 25-28, 2010, Dresden, Germany, pp. 328.

[6] D. C. Ni and C. H. Chin, "Classification on Herman Rings of Extended Blaschke Equations", Differential Equations and Control processes, Issue No. 2, Article 1, 2010. (http://www.neva.ru/journal/j/EN/numbers/2010.2/issue.html).

[7] D. C. Ni, "Numerical Studies of Lorentz Transformation", Proceeding of 7th EASIAM, Kitakyushu, Japan, June 27-29, 2011, pp. 113-114.

[8] D. C. Ni, "Entropy Computation On the Unit Disc of A Meromorphic Map", Journal of Applied Analysis and Computation, Volume 2, Number 2, May 2012 pp. 193-203.

[9] D. C. Ni, "Statistics constructed from N-body systems", Proceeding of World Congress, Statistics and Probability, Istanbul, Turkey, July 9-14, 2012, pp. 171.

[10] D. C. Ni, "Topological Transitions of Meromorphic Maps of Extended Lorentz Transformation", Proceeding of 8th EASIAM, Taipei, Taiwan, R.O.C., June 25-27, 2012, Article 12D.